Desalination and Water Treatment
www.deswater.com

doi: 10.5004/dwt.2019.24429

159 (2019) 93–109
August

The removal of fluoride from aqueous solutions using biomass ash derived from power industry

Anna Zdunek[a], Dorota Kołodyńska[b], Krzysztof Borowik[a,*], Piotr Rusek[a]

[a]*New Chemical Syntheses Institute, Al. Tysiąclecia Państwa Polskiego 13A, 24–110 Puławy, Poland, Tel. +48814731764; email: krzysztof.borowik@ins.pulawy.pl (K. Borowik), Tel. +48814731429; email: anna.zdunek@ins.pulawy.pl (A. Zdunek), Tel. +48814731473; email: piotr.rusek@ins.pulawy.pl (P. Rusek)*
[b]*Maria Curie-Skłodowska University, pl. M. Curie-Skłodowskiej 2, 20–031 Lublin, Poland, Tel. +48815375770; email: d.kolodynska@poczta.umcs.lublin.pl*

Received 29 November 2018; Accepted 18 May 2019

ABSTRACT

The ability of biomass ash to remove fluoride from aqueous solutions has been described. Seven samples of biomass ash from Polish power stations and combined heat and power plants using only biomass were tested as adsorbents for fluoride removal. After preliminary research, two of ash samples were chosen for further examination. Selected ash samples were examined in terms of the specific surface area and the pore size distribution. Their pH values of the point of zero charge were also determined. The examination of changes in the crystallographic phases of the sorbent before and after the sorption process was done using the XRD technique. Changes in ash samples before and after contact with the fluoride solution using the FTIR method were also analyzed. The effect of initial concentration of fluoride solutions, ash dose, contact time, temperature, pH, agitation rate and particle size of ash samples on fluoride removal efficiency has been examined. The percentage removal of the fluoride described as removal efficiency and the amounts of fluoride adsorbed per mass unit of ash vs. time and after reaching equilibrium was calculated. It was found that only in the case of one of the ash samples, CaF_2 was identified, and that probably has been precipitated as the result of that ash dissolution in water with the content of fluorides. The presence of fluorides in the residual solid phase bounded with compounds containing potassium, calcium sulphates and phosphates indicates that precipitation of CaF_2 is not the major mechanism responsible for fluoride removal. Therefore, an attempt was undertaken to describe the mechanism of the adsorption phenomenon. The kinetic profile of fluoride uptake was determined and the fitting to adsorption isotherm models was examined. The exact fitting to the pseudo-second-order model pattern of this model was confirmed for both of ash samples. It was found out that the fluoride adsorption process is well-described by Temkin isotherm plot.

Keywords: Fluoride; Biomass ash; Adsorption

1. Introduction

Fluoride ions are commonly known as chemical agents that cause health problems when their concentration in drinking water exceeds permissible limit which is set to be 1.5 mg L^{-1} (according to World Health Organization) [1]. On the one hand, their presence in a small amount is needed to maintain a proper condition of teeth, but on the other hand fluoride ions are very harmful to human health, if they are contained in food and drinking water. There are numerous articles describing the importance of fluoride in water and the causes of excess fluoride ions in water [2–4].

* Corresponding author.

Presented at the 6th International Conference on Sustainable Solid Waste Management (NAXOS 2018), 13-16 June 2018, Naxos Island, Greece.

The other sources of environmental pollution with fluorides are industrial processes, e.g., the metallurgical industry [5]. In this case, the fluoride presence in gaseous or wastewaters streams and their harmful impact on the particular parts of production plants is the main reason of the necessity for their removal. The presence of fluoride ions in operational solutions can cause very serious corrosion problems which are reflected in considerable damage of construction materials, depending on the kind of other solution components, pH and temperature in particular. Therefore, the removal of fluorides from these solutions is very important and what is more, because of its complexity, removing the fluoride ions from such systems is much more difficult than in the case of water.

Various techniques of defluoridation such as coagulation and precipitation, reverse osmosis, nanofiltration, electrolysis and electrodialysis, membrane processes, ion-exchange, Donnan dialysis, and adsorption have been used to reduce the excess fluoride [6,7]. Of all the fluoride removal methods mentioned above, the precipitation and adsorption appear to be much more cost-effective methods as compared with others. The adsorption method seems to be one of the most suitable techniques for the defluoridation as it is economical, environmental friendly and efficient, without the necessity of precipitated sludge removal and with the possibility of using the waste materials as sorbents. If regeneration of adsorbent material is possible, the cost of fluoride removal process is even lower. An additional advantage of the sorption method is that it can be realised in two ways, in a static system, by addition of adsorbent to the reactor and filtration of fluoride loaded material and in a dynamic system with the flow of the purified solution through a bed filled with adsorbent material. Numerous kinds of adsorbents have been reported to be effective for fluoride adsorption such as: activated carbon, activated alumina, calcite, tricalcium phosphate and activated soil sorbents [8]. Considering the fluoride removal from wastewaters, when the quality of solution obtained is not as important as in the case of drinking water, it is advisable to use inexpensive materials to remove fluorides, especially waste materials, so as not to increase the operating costs of the purification process. Various types of inexpensive sorption materials for fluoride removal, called low cost type sorbents, described in the literature which includes alum sludge [9,10], red mud [11,12], coal mining waste [13,14], spent catalyst [15,16], electrocoagulation sludge [17], coal fly and bottom ash derived from power station [18,19].

Coal fly ash is one of the major industrial solid wastes and its amount increases year by year all over the world. Therefore, recycling of coal fly ash is of a great concern. Fly ash has been used as an efficient adsorbent for the removal of various pollutants [20]. Since the surface has an anionic charge, the anion species adsorption capacity of fly ash is very low but this problem can be solved by modifying the external surface of fly ash with cationic coatings for the improvement in anion exchange capacity [21]. There have been also studies carried out concerning the use of coal ash as fluoride adsorbent material [22,23]. The main components of coal fly ash are silicon, aluminum and iron oxides. There are also variable amounts of carbon, calcium, magnesium and sulphur [24]. Coal fly ash is a material with a hydrophilic surface and porous structure. Fly ash particles are predominantly spherical in shape and contain irregular fragments that are mainly made of unburnt carbon, anhydrite and calcite. Physical and chemical properties of coal fly ash depend on combustion conditions, collector setup, boiler types and gas emission control system [25]. The adsorption capability of coal fly ash depends mainly on physical and chemical properties such as particle size, surface area and pH. Since the surface of fly ash has a negative charge, the adsorption capacity of anion species is very low [26] and therefore, some modifications are required. The studies described [27] present test results on fly ash used for fluoride removal from water and wastewaters instead of expensive adsorbents such as activated carbon, activated alumina, activated bauxite, and so on. In general, the use of coal fly ash as fluoride sorbents requires its thermal or chemical modification of ash. Without any modification, the fluoride sorption capacity for coal fly ash is low, and depending on the initial fluoride concentration from 5 to 15 mg L^{-1}, it increases from 0.2240 to 0.6150 mg g^{-1} [28]. Low capacity causes the necessity of using the large dosage of coal fly ash. Only after a chemical modification, the sorption capacity of coal ash increases.

Besides the coal ash, energy and heating sector of industry generates some amounts of ash derived from biomass combustion. The interest in biomass including wood biomass, for energy purposes has been growing in recent years in Poland, which confirms that power plants and heat-generating plants are obliged to co-burn biomass with coal, and some of them have installed boilers fed with biomass only. In Poland, the power industry is focused mainly on the consumption of domestic resources of hard coal and brown coal, which are considerable and assure a high level of energy safety. However, at the same time, meeting the requirements specified in the Climate and Energy Package of the European Union, especially in the frame-work directive on the promotion of the use of energy from renewable sources [OJ EC L 140 2009], makes the use of energy carriers, other than natural minerals are very important. Biomass combustion is beneficial due to the reduced use of fossil fuels and the achievement of CO_2 emission targets, and because of the lowered SO_x and NO_x emissions as compared with coal combustion [29]. Despite some disadvantages associated with biomass combustion process itself which were identified at the same time, the increase in the amount of biomass burned is anticipated for the purpose of reducing the amount of coal combusted. Therefore, there is also necessity to utilize the ash obtained after biomass combustion or co-combustion with coal.

The chemical composition of biomass fly ash is much more variable than that of coal ash. The composition of coal fly ash varies in a wide range, but the dominant components are silicates or aluminosilicates. The diversity of chemical composition of biomass ash is very high not only due to the type of vegetation, but also because of soil conditions influencing vegetation growth and soil composition. Some of them are rich in potassium and magnesium phosphates, other rich in carbonates (e.g., calcite, fairchildite, kutnahorite), sulphates (arcanite) and lime beside other components as quartz or cristobalite, and iron oxides [30].

When comparing the composition of coal and biomass fly ash, it can be concluded that they differ mainly in the content of constituents such as Al_2O_3, Fe_2O_3, CaO, K_2O, P_2O_5 and SO_3

as well. A higher content of CaO in biomass ash suggests that they may be more effective fluoride ion sorbents than coal fly ash. In addition, they also contain up to several percent of phosphorus which in combination with calcium creates compounds capable of binding fluorine, as it is found in phosphoric minerals, such as fluorapatite. Due to the content of some components in biomass ash which can bind fluorides, studies of fluoride sorption using this kind of ash were carried out.

In the literature reports, there are studies described concerning the use of biomass and biomass ash for fluoride removal. Biomass used for fluoride removal in these studies includes rice husk [31], fresh leaves from neem, pipal and kikar trees [32], seeds [33,34], pineapple peel powder [35], banana peel [36] or pine wood char [37]. Using the ash from various kinds of biomass formed, as the result of intentional combustion of some kind of biomass such as leaves [38], maize husk [39,40], tea [41], rice husk [42,43] is described in literature. Fluoride adsorption capacity of these types of biomass and biomass ash is different for every type of material. Studies on the fluoride removal using leaves from trees with and without chemical treatment showed that 10 g L^{-1} of adsorbent dose for 50 mL sample volume with 15 mg L^{-1} of fluoride ion concentration reduced the content of fluoride to 0 mg L^{-1} within 180 min at 29 ± 0.5°C. It was observed that approximately 80% removal was achieved within 60 min of the contact time. The experimental data fitted well with Langmuir adsorption isotherm [44]. In the case of seeds, for tamarind seeds, an adsorption capacity of 6.37 mg g^{-1} at 20°C was achieved and the defluoridation followed first order kinetics and Langmuir adsorption isotherm [33]. In studies on the removal of fluoride from aqueous solution by mechanically modified guava seeds from water in batch mode, the experimental data obtained fitted well for pseudo-second-order kinetic model and Langmuir-Freundlich isotherm model indicating that fluoride adsorption was characterized by chemisorption on heterogeneous surfaces [34]. The obtained adsorption capacity was 15.6 mg g^{-1}. The fluoride adsorption capacity for ashes is much higher than for unburned biomass. For example, for the rice husk ash, the fluoride adsorption capacity of adsorbent was 15.08 mg g^{-1} in batch and 9.5 mg g^{-1} in column study. The maximum fluoride removal was achieved for pH 5.0 ± 0.5 and it showed that adsorption was not dependent on initial fluoride concentration. Freundlich isotherm with multilayer adsorption and pseudo second order kinetic were best fitted [45]. In the case of tea ash, Al/Fe loaded oxides tea waste was used for the removal of fluoride from drinking water. The bio-adsorbents with tea-Al and tea-Al-Fe were able to reduce the fluoride below 1.5 mg L^{-1} with an optimum pH range of 4.0–8.0 and contact time of 2 h. The defluoridation capacity of original tea, tea-Fe, tea-Al and tea-Al-Fe were 3.83, 10.47, 13.79 and 18.52 mg g^{-1}, respectively. The experimental data fitted well with a Langmuir isotherm model for metal loaded tea waste, whereas, it followed Freundlich isotherm model for original tea waste. The adsorption process was followed by Lagergren pseudo-second-order kinetic model. The fluoride ions were adhered by positively charge surface sites in acidic phase and involved ligand exchange at pH > 6 [46].

Taking into account, the fact that there are studies describing the possibility of fluoride removal using the biomass or biomass ash mentioned above, it can be assumed that biomass ash obtained from power station and combined heat and power plants, could also be good material for fluoride removal, which is much more efficient than coal fly ash. Pursuant to legal regulations, the composition of biomass burnt to obtain energy is partially restricted by the energy law, because a composition of the biomass source is strictly defined with regard to the share of biomass from agricultural production residues or agrofood industry and wood biomass [47]. The agricultural biomass is the material that comes from agriculture and the processing industry of its products (straw, grain, energy plantations, e.g., energy willow, waste from the oil and food industry). The forest biomass means every material that comes from forest and the industry processing the raw material from the forest (sawdust, woodchips, logging waste and pulp mill).

To estimate the possibility of fluoride removal using biomass ash, originated from power station, studies on affinity of several ash samples to fluoride were carried out. The main object of this work is to find out if biomass ash, as the waste from the energy industry, can be used as material for fluoride removal, without any prior pre-treatment.

2. Experimental setup

2.1. Sorbents characterization

Fluoride ion sorption tests were carried out using biomass fly ash samples. Fly ash samples were collected from seven Polish power and the combined heat and power plants. All of them came only from biomass combustion. The burned biomass consisted mainly of wood biomass (coniferous and deciduous tree) with the addition of agricultural residues. All fly ash samples were characterized by X-ray fluorescence (XRF) analysis (X'Unique II, Philips) to determine the concentration of main components. In order to obtain a general knowledge about the affinity of the fly ash sample to fluorides, the preliminary tests for each ash sample were carried out. To ensure maximum sorption capacity, a very small amount of every fly ash sample (0.5 g) was added to 50 mL of a highly concentrated fluoride solution (5 g L^{-1}) and left on a magnetic stirrer for 15 h. After this period of time, the fluoride concentration was determined. From the pre-tested ash samples, two with the highest affinity for fluoride ions were selected for further research.

In order to better understand the mechanism of fluoride uptake, XRD analyzes (PANalytical Empyrean) of ash samples were carried out to identify the morphological structure and crystallinity range of the ash, before and after fluoride binding.

The Fourier-Transform infrared spectroscopy (FTIR) analysis was also performed to understand the spectroscopic features of the biomass fly ash and to gain in-depth knowledge of the mechanism of fluoride binding by these ash samples. Infrared spectra were measured using a Nicolet iS10 spectrometer produced by Termo Scientific. The spectra were recorded using the appropriate ATR technique (attenuated total reflection) at room temperature with 4 cm^{-1} resolution in the mid-infrared spectral range of 400–4,000 cm^{-1}.

In order to assess the surface charge of the biomass fly ash as is shown in relation to the solution, depending on the pH of this solution, the value of pH_{PZC} was determined. The pH value above which the total surface of the biomass fly ash samples particles are negatively charged, i.e., pH of the point of zero charge (pH_{PZC}), was determined according to method described in [48]. It was carried out by measuring the suspension pH, obtained by mixing 0.2 g of ash with 50 mL of a 0.05M NaCl solution with various pH values in a container with a cup for 24 h. The initial pH was adjusted to values between 2 and 12 by adding either 0.1M solution HCl or 0.1M NaOH solution. The final pH (pH_e) after 24 h was measured and the difference between this value and pH of the initial solution was plotted against the initial pH. The pH value for which the curve crosses the line that correspond of $pH_e–pH_0 = 0$, was taken as the pH_{PZC} of the biomass fly ash.

In order to obtain the porous structure characteristic of biomass fly ash samples, the nitrogen adsorption-desorption isotherm was determined. The specific surface area of ash was determined by Brunauer-Emmett-Teller (BET) method and a pore size distribution was determined according to Barret-Joyner-Halenda (BJH) model. The specific surface area was determined by means of the nitrogen adsorption method at the temperature of liquid nitrogen –196°C) using a Micromeritics ASAP (accelerated surface area and porosimetry system) 2050 analyzer (USA). The fly ash samples, in the amount of approximately 2 g were subjected to degasification in order to reach the pressure of 10 mmHg at the 80°C temperature. Measurement data approximation to the BET equation was made using the computer software coupled with the analyzer, its coefficients were determined and the specific surface area was calculated in the range of relative pressure p/p_0 = 0.05–1.0. The pore volume and pore size distribution, in the pore size ranging from 2 to 300 nm (according to producer declaration), were determined from N_2 adsorption isotherm in the p/p_0 = 0.02–0.99. However, the real maximum diameter of pores that were measured was not higher than 250 nm.

Particle size distribution of selected fly ash samples was measured using a laser particle size analyzer (Mastersizer 3000, Malvern) to check the variability of grain size.

2.2. Methods

2.2.1. Batch study

All fluoride removal tests were carried out in batch mode in plastic containers of 100 mL capacity with caps. All experiments were conducted in aqueous solution of ammonium fluoride. Fly ash in the amount of 0.5 g (except the investigations of ash dose effect) was added to 50 mL of fluoride solutions of a desired concentration. After placing the solutions and fly ash in the containers, these containers were closed and immediately placed in a multi-station magnetic stirrer (IKA WERKE RT 10 power) at 550 rpm at room temperature, unless otherwise stated. The contact time of the solid phase with the solution was 15 h (except for time and temperature influence studies), to obtain a thermodynamic equilibrium. Each time a set of the stirring bars with the same shape and size was used. Only the temperature effect tests were carried out in slightly different conditions. In this case, the fluoride solutions were placed in plastic bottles with caps and they were shaken for 30 min in a water bath orbital shaker to obtain desired temperature. Considering that the conditions of solid phase contact with the solution are different, depending on the type of mixing machine was used, the temperature effect was evaluated in relation to the results obtained under the same conditions but at the ambient temperature. After the desired contact time of the liquid and solid phases, these phases were separated using vacuum filtration kit equipped with Whatman No-42 filter paper. Then, 25 mL of each filtrate was taken for analysis to check the fluoride concentration in the aqueous solution. All experiments were repeated three times. The values given are the average value calculated on the basis of the results obtained.

2.2.2. Preparation of stock solution

It was assumed that the main form of fluoride in these solutions is ammonium fluoride. Therefore, all the experiments described in this article have been conducted using solutions of ammonium fluoride (Acros Organics, Belgium), pure for analysis grade. Before preparing the desired concentration of solution, ammonium fluoride was dried at 343 K temperature to ensure removal of moisture and to prevent against degradation of ammonium fluoride which occurs at 373 K [49].

2.2.3. Analytical methods

The fluoride concentrations in the test solutions were measured by the direct potentiometric method. A fluoride selective electrode, Monokrystaly 09–37 type, made of lanthanum fluoride single crystal (LaF_3) was used as the indicating electrode combined with the AgCl electrode used as the reference one. A citrate buffer was used to maintain the required pH value demanded for linear relationship between the measured signal and $\log_{10}$ of molar concentration of standard fluoride solutions. Standard fluoride solution of 1,000 mg F/L were prepared by dissolving 2.21 g sodium fluoride (Acros Organics) (dried at 353 K) in 1,000 mL volumetric flask and make the volume up to mark with ultrapure water from Milli-Q ultrapure water system. The experimental solutions of desired concentrations were prepared by diluting the standard solution.

2.2.4. Theoretical and mathematical formulations describing the fluoride adsorption process

It should be assumed that the dominant mechanism casing fluoride binding by fly ash from biomass is the adsorption process. The main parameters describing the adsorption process have been calculated.

The percentage removal of the fluoride described as removal efficiency (% R) was calculated using the following equation:

$$\%R = \frac{c_0 - c_t}{c_0} \times 100 \quad (1)$$

where c_0 and c_t are the initial and at time t fluoride concentrations in working solution respectively, in mg F^-/L.

The amounts of fluoride adsorbed per mass unit of fly ash at any time t (q_t, mg g^{-1}) and the amounts of fluoride removed after reaching equilibrium (q_e, mg g^{-1}), were calculated as follows:

$$q_t = \frac{(c_0 - c_t)}{m} \times V \tag{2}$$

$$q_e = \frac{(c_0 - c_e)}{m} \times V \tag{3}$$

where c_e is the equilibrium fluoride concentration in working solution, in mg F^-/L and V is the volume of fluoride ions solution, L.

The kinetics of fluoride adsorption was modeled using the Lagergren's pseudo-first-order model (PFO) (Eq. (4)), the pseudo-second-order model (PSO) developed by Ho and McKay (Eq. (5)) and the intraparticle diffusion model (IDP) proposed by Webber and Morris (Eq. (6)). The following equations were used:

Pseudo-first-order model

$$\ln (q_e - q_t) = \ln q_e - k_1 t \tag{4}$$

Pseudo-second-order model

$$\frac{t}{q_t} = \frac{t}{q_e} + \frac{1}{k_2 q_e^2} \tag{5}$$

Intraparticle surface diffusion model

$$q_t = k_i t^{1/2} + C \tag{6}$$

where k_1 and k_2 are the rate constants of pseudo-first-order and pseudo-second-order adsorption expressed in min^{-1} and in g/mg·min, respectively, k_i is the intraparticle diffusion rate constant expressed in mg/g·$min^{1/2}$, C is the intercept.

The values of rate constants were determined from the slope of the linear plot. The conformity of the predicted values with the experimental data was evaluated based on the value of correlation coefficient R^2.

In order to describe the nature of interaction of fluoride and fly ash, the adsorption isotherm models were applied. The obtained experimental values were fitted to the adsorption equations which are most commonly used to characterize the adsorption process from solutions i.e., Langmuir isotherm (Eq. (7)), Freundlich isotherm (Eq. (8)) and Temkin isotherm (Eq. (9)). These models were described by equations as follows:

Langmuir isotherm

$$\frac{1}{q_e} = \frac{1}{K_L q_t c_e} + \frac{1}{q_t} \tag{7}$$

Freundlich isotherm

$$\ln q_e = \ln K_F + \frac{1}{n} \ln c_e \tag{8}$$

Temkin isotherm

$$q_e = B_T (\ln A_T + \ln c_e) \tag{9}$$

where K_L is the Langmuir constant related to the binding energy or affinity parameter, K_F is a Freundlich constant connected with the sorption capacity, n is the Freundlich constant connected with the adsorbate and adsorbent affinity, B_T is the Temkin constant related to the heat of adsorption, A_T is the Temkin equilibrium binding constant corresponding to the maximum binding energy.

3. Results and discussion

3.1. Characterization of the biomass fly ash

The XRF analysis of biomass fly ash samples has demonstrated a variety of the major components in respect of their chemical composition (Table 1). Some of them are rich in silica with the content higher than 50% (AB 3, AB 4) while other samples have the silica content ranging from 15% (AB 1, AB 5) to almost 40% (AB 6, AB 7). This variability of the silica content indicates differentiation of the solubility of these ash constituents in water. This feature is important especially for using this fly ash for fluoride removal only from aqueous solutions. AB 1 and AB 2 contain about 25.9% and 19.3% CaO respectively, while the rest of samples contain about 15% of CaO. The highest P_2O_5 content was found in the fly ash AB 1, AB 2 and AB 5. Fly ash AB 2 and AB 5 have higher content of K_2O than the other. The AB 6 and AB 7 fly ash samples contain much more Al_2O_3 and Fe_2O_3 than the other fly ash. It has been also noticed that the examined fly ash samples differ in terms of the quantity of loss of ignition that means that the quantity of inorganic and organic carbon is different.

As the result of the preliminary research (Fig. 1), fluoride removal efficiency with over 20% was achieved for the following fly ash samples AB 1, AB 2, AB 3 and AB 6. Lower ability of fluoride removal was obtained for fly ash samples AB 4, AB 5 and AB 7, when the removal efficiency was between 10% and 20%. The AB 4, for which the removal efficiency value was just about 11%, showed the lowest affinity to fluoride. Of the of all the fly ash samples examined, AB 1 and AB 2 were chosen for further research.

The most important components of ash used for fluoride removal are those that contain Ca, Mg, Al, Fe, and Si. The obtained results reveal an ability to fluoride binding, the main phases containing these elements were specified in accordance with the XRD pattern (Figs. 2 and 3). It was revealed that the major crystal phases of both of examined fly ash are SiO_2 (ICDD 1-70-7344) and $CaCO_3$ (ICDD 1-80-9775), but they also have a high content of β-K_2SO_4 (ICDD 4-7-2698/4-6-8317) and KCl (ICDD 1-74-9685). Among the dominant phases of AB 1 ash sample, $CaSO_4$ (ICDD 37-1496) and $K_2Ca(SO_4)_2 \cdot H_2O$ (ICDD 28-739) can also be found. The minor phases of that ash are $Ca(OH)_2$ (ICDD 4-8-220) and

Table 1
Chemical composition of ash samples, the losses of ignition and water insoluble part content

Parameter	Content in ash samples, % w/w						
	AB 1	AB 2	AB 3	AB 4	AB 5	AB 6	AB 7
CaO	25.89	19.34	15.15	14.16	16.45	14.98	14.54
SiO_2	14.25	18.96	56.40	56.09	15.00	36.78	36.06
P_2O_5	4.88	3.40	2.10	1.81	3.02	1.30	0.26
Al_2O_3	3.62	2.43	2.78	2.86	1.74	16.96	19.95
MgO	2.69	3.04	2.90	1.98	3.32	2.75	2.71
Fe_2O_3	2.09	2.23	2.08	1.06	1.49	7.78	5.81
SO_3	15.11	13.71	2.52	1.54	10.85	7.66	4.76
K_2O	10.08	20.53	6.57	4.68	16.33	3.34	1.89
ZnO	2.42	0.26	–	0.10	0.26	0.10	–
TiO_2	0.17	0.16	0.16	0.16	1.70	1.19	0.78
Mn_2O_3	0.97	0.68	0.51	0.53	0.72	0.13	0.16
Na_2O	1.06	1.46	1.02	0.8	3.75	1.09	1.80
Loss of ignition (1273 K)	15.05	12.52	6.84	10.09	20.16	5.65	10.93
Water insoluble part	80.18	68.95	90.62	93.77	55.92	95.63	91.11

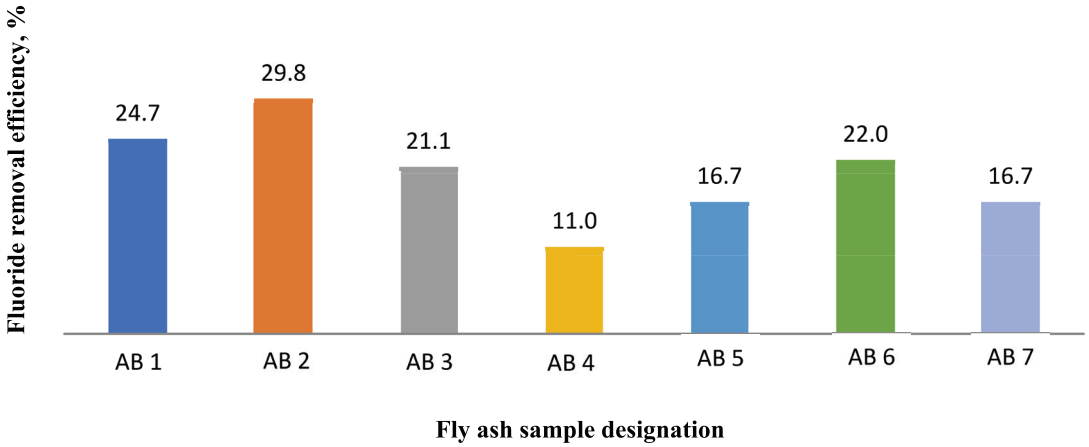

Fig. 1. Results of the preliminary research on removal efficiency of fluoride using seven fly ash samples (50 mL of 5 g F^-/L solution; 0.5 g of fly ash; 15 h of contact time; 550 rpm of agitation speed (magnetic stirrer); ambient temperature).

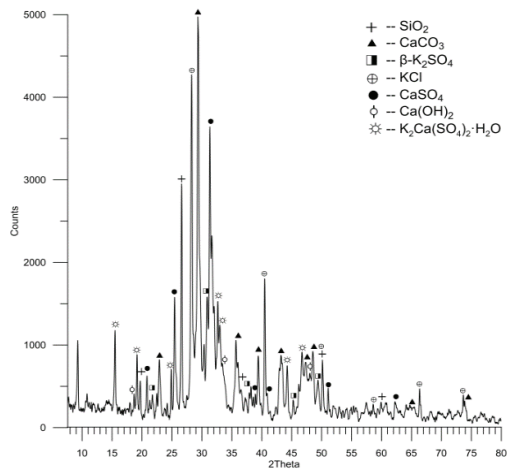

Fig. 2. XRD analysis of AB 1.

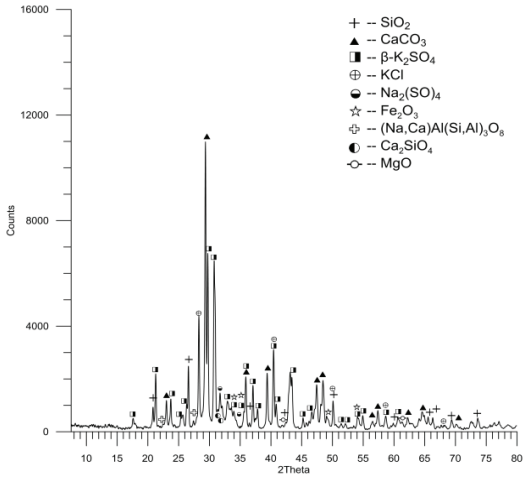

Fig. 3. XRD analysis of AB 2.

$Mg_xFe_{1-x}SiO_3$ (ICDD 4-16-5580). The phases such as Na_2SO_4 (ICDD 4-10-4862), Fe_2O_3 (ICDD 4-16-4345/4-3-2900), (Na, Ca) $Al(Si, Al)_3O_8$ (ICDD 41-1480), Ca_2SiO_4 (ICDD 24-234) and MgO (ICDD 4-6-6924/4-8-8202) are among the minor phases of AB 2 ash sample. The presence of such phases like $K_3H(SO_4)_2$ (ICDD 1-79-7286) and K_2HPO_4 (ICDD 25-639) cannot be excluded but it is impossible to confirm their presence in this fly ash because of the overlap of the peaks.

The results of XRD analysis of the residue obtained on the filter paper, after the separation of fluoride solution and the fly ash are shown in Figs. 4 and 5. Among the phases containing the fluoride, K_3SO_4F (ICDD 43-229) was recognized in both fly ash samples. The phase of $Ca_5(PO_4)_3F$ (ICDD 4-14-8746) has been identified in AB 1, in a little bit higher amounts than the last phase. In the case of the AB 2 ash sample, the fluoride containing phases such as CaF_2 (ICDD 4-7-1254) and $Ca_5(PO_4)_3(OH)_{0.8}F_{0.2}$ (ICDD 4-16-2908) were recognized.

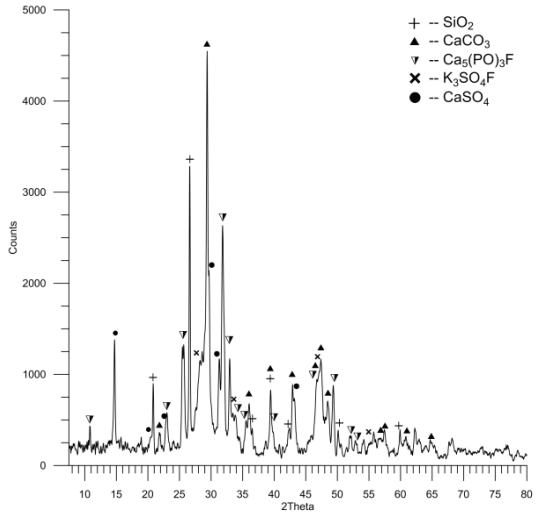

Fig. 4. XRD analysis of AB 1 after contact with fluoride solution.

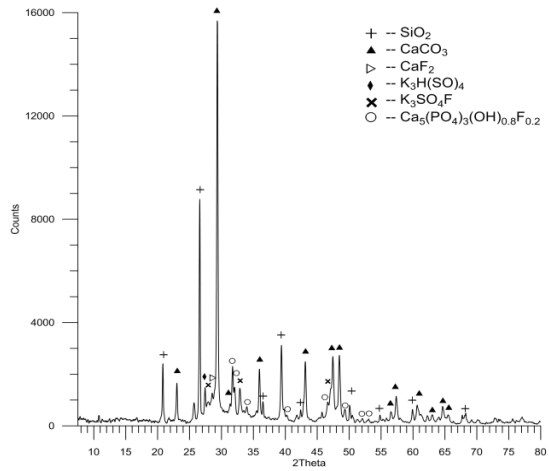

Fig. 5. XRD analysis of AB 2 after contact with fluoride solution.

The FTIR spectra obtained for AB1 and AB 2 biomass ash samples before and after contact with fluoride solution are presented in Figs. 6 and 7. The FTIR spectra of the biomass fly ash samples show the presence of the band around 3,330–3,400 and 1,414, 1,413 cm^{-1} related to the stretching vibration of H_2O and structural O-H groups of the fly ash, indicating the presence of surface hydroxyl groups and physically adsorbed water. In the case of AB 1, there are bands at 1,137 and 1,123 cm^{-1} detected, which can be related to vibration of C-F bond (it is probably due to presence of trace amounts of fluorine compounds in fly ash). A band at 1,101 cm^{-1} was related to the stretching vibrations of the groups Si-O and the band at 1,032, 1,035, 1,047 cm^{-1} was related to Si-O-Si bending vibrations. There are also bands at 876 and 874 cm^{-1} detected, related to the bending vibration of Si-H and stretching vibration of Si-O. After contact of biomass ash samples with fluoride solution, the bands at 1,640 and 1,413–1,414 cm^{-1} indicate the formation of N-O in the washing process of the fly ash because of ion exchange. At 1,035 and 1,032 cm^{-1} there are asymmetric stretching vibration of Si-O-Si detected which weren't visible in biomass fly ash samples before contact with fluoride solution. There are also bands at 875 and 874 cm^{-1} related to the SiF, SiF_2 bonds. In the case of AB 2 ash sample after fluoride loading, there are also slight bands noticeable at 2,511 and 1,796 cm^{-1} probably related to the bonds present in calcium carbonate [50]. As it has been reported in [51] the bands occurring at 1,000–1,100, 1,100–1,300 cm^{-1} and around 879 cm^{-1} can also correspond to the presence of carbonates.

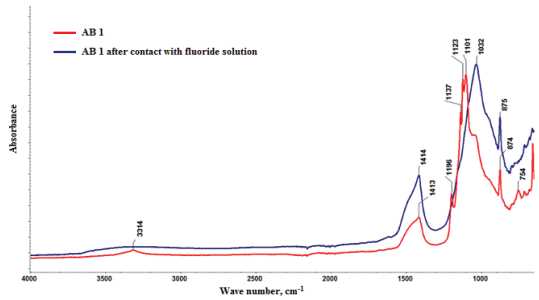

Fig. 6. FTIR spectra of AB 1 before and after contact with fluoride solution.

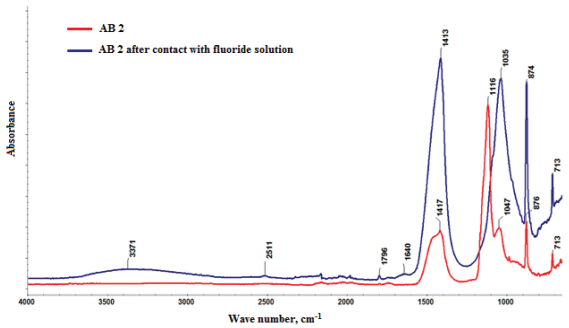

Fig. 7. FTIR spectra of AB 2 before and after contact with fluoride solution.

From Fig. 8 it can be observed that the biomass fly ash samples differ from each other by the pH_{PZC} value. The biomass fly ash AB 1 shows positive charge of the surface below the 7.7 of solution pH and above this value it is negatively charged. When the pH increases to about 12, the charge of surface is positive again, whereas, in the case of biomass fly ash AB 2, it is positively charged for all the initial pH range. Only increasing the initial solution pH to the 12.7 value allowed the determination of pH_{PZC} as 12.02. For the values lower than pH_{PZC}, the phenomenon of fluoride ions bounding is connected with the reaction with positively charged cations such as Ca^{2+}, Mg^{2+} or Al^{3+}. For the pH higher than pH_{PZC}, the mechanism of fluoride removal is due to exchange with other anions such as OH^-. The mechanism of fluoride removal using each of biomass fly ash samples is the same for the pH lower than 7.7 and for values higher than 12, because both ash samples are positively charged for that range of pH. Therefore, the nature of fluoride removal process using biomass fly ash examined depends on the ionic strength of the solution containing fluoride ions and the fluoride removal efficiency will vary for the various values of solutions pH.

Parameters describing porous structure of biomass fly ash samples obtained from the sorption isotherms by means of BET (Figs. 9 and 11) and BJH (Figs. 10 and 12) transformation are presented in Table 2.

According to the IUPAC classification [52], each of the obtained adsorption-desorption isotherms (Figs. 9 and 11) has a similar shape to the type IV of isotherm which is characteristic of mesoporous materials. The shapes of hysteresis are similar to the type H3 of hysteresis loops. The shapes of hysteresis loops were often identified with specific pore structures. The type H3 loop is observed with aggregates of plate-like particles giving rise to slit-shaped pores [52].

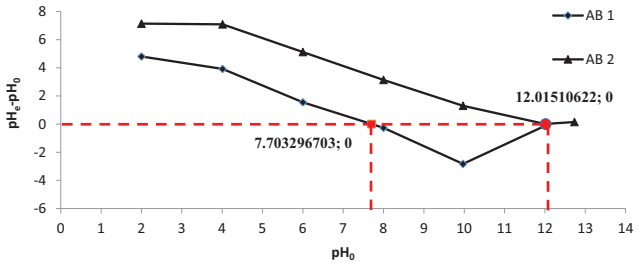

Fig. 8. Determination of the pH_{PZC} for AB 1 and AB 2

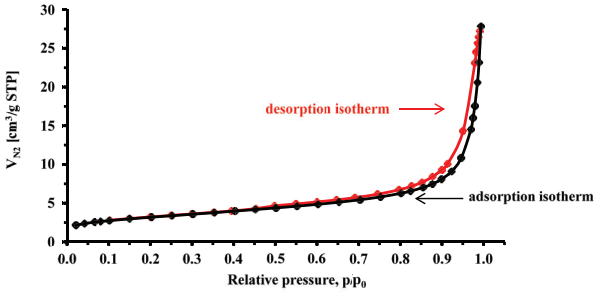

Fig. 9. Adsorption-desorption isotherms for the AB 1.

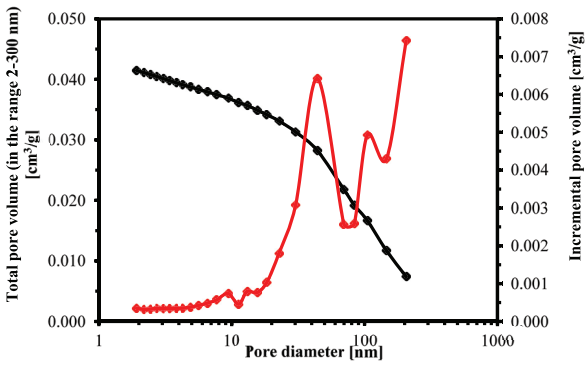

Fig. 10. Pore size distribution of AB 1.

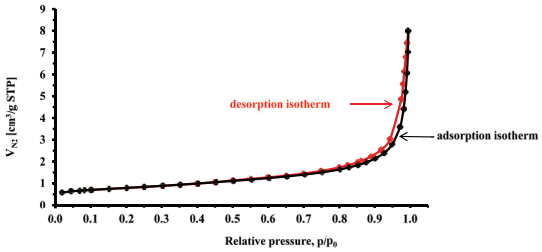

Fig. 11. Adsorption-desorption isotherms for the AB 2.

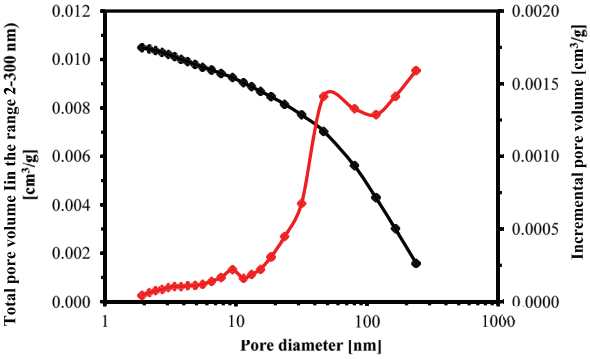

Fig. 12. Pore size distribution of AB 2.

Table 2
Textural parameters of biomass fly ash samples determined by low-temperature nitrogen adsorption isotherms

Biomass ash sample	AB 1	AB 2
S_{BET}, $m^2\ g^{-1}$	11.1	2.7
V_t, $cm^3\ g^{-1}$	0.041	0.01
V_{mez}, $cm^3\ g^{-1}$	0.02	0.005
d_a, nm	20.088	20.394

S_{BET}: the size of the specific surface area determined by BET method;
V_t: the total pore volume, in the range 2–300 nm (2–205 and 2–237 nm for AB 1 and AB 2 respectively) determined with BJH method;
V_{mez}: the volume of mesopores (2–50 nm) determined by BJH method;
d_a: the average pore diameter.

The biomass ash samples differ in the size of the specific surface area. The specific surface area of AB 1 fly ash sample (11.1 m^2 g^{-1}) is four times greater than of AB 2 (2.7 m^2 g^{-1}). Nevertheless, the size of the specific surface area for both ash samples is much higher than in the case of coal fly ash for which S_{BET} is 0.44 m^2 g^{-1} [53] but much lower than for active carbon for which S_{BET} is 1,425 m^2 g^{-1} [54].

The total pore volume in the range of measurement, i.e., 2–205 nm for AB 1 and 2–237 nm for AB 2, is 0.041 and 0.01 cm^3 g^{-1} for AB 1 and AB 2, respectively, 0.02 cm^3 g^{-1} for AB 1 and 0.005 cm^3 g^{-1} for AB 2 of which are mesopores (>2 and 50> nm according to the IUPAC terminology [55]). As it can be seen in Figs. 2 and 4, some micropores (<2 nm) were also detected, as well as macropores, with pore diameter of approximately 80 nm and greater for AB 1 and of approximately 120 nm for AB 2, for the biomass ash samples examined. The average pore diameter is 20.088 and 20.394 nm for AB 1 and AB 2 biomass ash samples, respectively.

Based on the comparison of particle size distribution of fly ash samples (Figs. 13 and 14) it can be noticed that the value of median $D_v(50)$ for both fly ash samples is almost the same and it is about 6 μm. The value of $D_v(10)$ is also very similar for both fly ash samples. The main difference between the two examined fly ash samples concerns the value of $D_v(90)$. Less than 90% of AB 1 particles in volume share are lower than about 22 μm, whereas in the case of AB 2, they are lower than 70 μm. The AB 2 fly ash sample contains some amount of much bigger particles than the AB 1 fly ash sample but about 50% of the volume fraction is of almost the same size.

3.2. The effect of experimental parameters

To obtain a general view of the possibility of biomass fly ash used for fluoride removal from aqueous solutions, the series of experiments with a different types of variable parameters were carried out. The initial concentration of fluoride solution, the fly ash dose and the contact time of solid and liquid phase have been considered to be the most important factors. Considering several various kinds of materials that show the ability to remove some contaminants, the determination of minimal dose and time needed to obtain satisfactory results seems to be the most important thing for assessing their usefulness. The selection of the type of removing material should be primarily economically justified. If less amount of such material is needed and the assumed aim is achieved more quickly, such material is regarded as having better properties. It is also important to know for which concentrations of contaminants that the material is effective. Some removal materials are suitable for solutions with a lower concentration of impurities but the other is effective for higher values only.

In order to obtain more information, the effect of temperature, pH, agitation speed and a particle size of fly ash were also examined. The effect of each parameter on fluoride removal efficiency was discussed in detail below. In all the cases, the removal efficiency and the amount of fluoride adsorbed per mass unit of ash were evaluated.

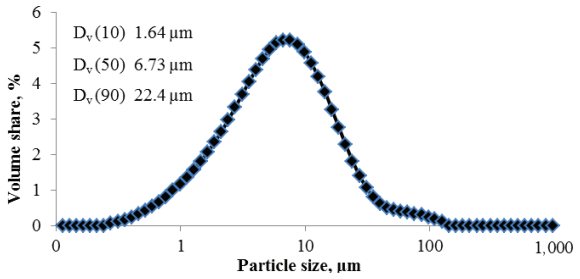

Fig. 13. Particle size distribution of AB 1.

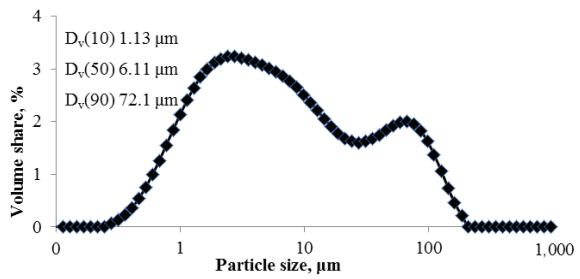

Fig. 14. Particle size distribution of AB 2.

3.2.1. Initial fluoride concentration

As it can be seen in Fig. 15 removal efficiency increases with the initial concentration of the fluoride solution from 0.05 to 0.5 g L^{-1}, but with fluoride concentration of 1 g L^{-1} and higher, the percentage removal of the fluoride decreases. Each of the fly ash samples exhibits a different effectiveness for every value of fluoride concentration. AB 1 fly ash sample is very effective for even very low fluoride concentrations for solutions of 0.05–0.5 g F^-/L with the removal efficiency ranging from 81.3% to 97.5%, respectively. For the same initial concentrations, the effectiveness of fluoride removal for the fly ash AB 2 is only from 14.5% to 45.3%. With the increase of fluorides, in case of AB 1 the removal efficiency and it decreases significantly and decreases slightly in case of AB 2. For fluoride concentration of 4 g L^{-1}, the removal efficiency of both fly ash samples is almost the same, and for 5 g L^{-1}, efficacy of the AB 1 is even lower than for AB 2.

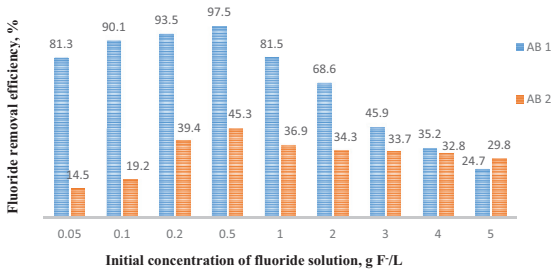

Fig. 15. The effect of initial concentration of fluoride solutions on removal efficiency by AB 1 and AB 2 (50 mL of solution; 0.5 g of ash; 15 h of contact time; 550 rpm of agitation speed (magnetic stirrer); ambient temperature).

The quantity of fluoride adsorbed per mass unit of ash increases for AB 1 with the increase of the initial solution, but it decreases above the fluoride content of 4 g L^{-1} (Fig. 16). In the case of AB 2 sample, the sorption capacity increases with the increase of initial fluoride concentration, which means that the sorption capacity of this fly ash is not fully loaded.

3.2.2. Adsorbent dose

For each initial fluoride concentrations that have been examined, increasing the fly ash dose caused the increase of the removal efficiency of AB 1 and AB. In the case of 0.05 g L^{-1} fluoride solution (Fig. 17), high removal efficiency of about 70% can be reached by using 0.3 g of ash per 50 mL for the AB 1. For AB 2, even 1 g of fly ash results in an increase in efficiency removal only slightly over 20%. The amount of fluoride removal per gram of fly ash decreases with the increasing dose of fly ash and it is a maximum of 5.8 mg g^{-1} for dose of 0.1 g and 4.8 mg g^{-1} for dose of 0.05 g, for AB 1 and AB 2, respectively (Fig. 18).

For the initial fluoride concentration of 0.5 g L^{-1} (Fig. 19), 0.3 g of AB 1 is sufficient to achieve 79.8% removal efficiency and to increase the dose to 1 g, resulting in removal efficiency up to almost 98%. For AB 2 and 0.1 g of ash is sufficient to achieve more than 20% removal efficiency, and the increase to 1 g causes the improvement of removal efficiency of over 60%. The amount of fluoride uptake per 1 g of ash increases with the ash dose increased from 0.05 to 0.1 g for AB 1, and then it decreases for larger amounts of fly ash, as it is in case of AB 2 (Fig. 20). The maximum value was over 74 mg g^{-1} and over 88 mg g^{-1}, for AB 1 and AB 2, respectively.

For the initial fluoride concentration of 1 g L^{-1} (Fig. 21), 0.5 g of fly ash is needed to obtain almost the same values of removal efficiency as for 0.3 g of fly ash, for the 0.5 g L^{-1} (Fig. 19). Increasing the fly ash dose to 1 g, allows to achieve the removal efficiency of 98.3% and 48.8% for AB 1 and AB 2, respectively. The amount of the fluoride uptake per 1 g of

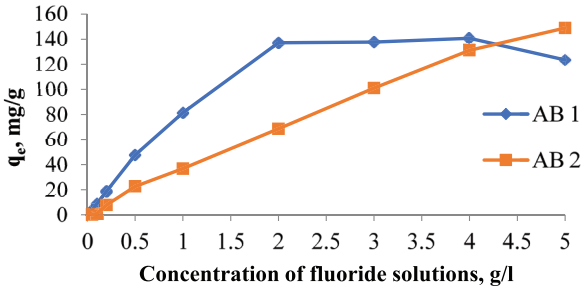

Fig. 16. The effect of initial concentration of fluoride solutions on equilibrium capacity of AB 1 and AB 2 (50 mL of solution; 0.5 g of ash; 15 h of contact time; 550 rpm of agitation speed (magnetic stirrer); ambient temperature).

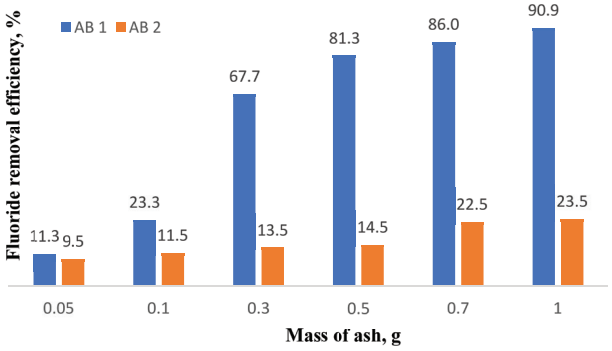

Fig. 17. The effect of fly ash dose on fluoride removal efficiency for solutions containing 0.05 g L^{-1} of fluoride (50 mL of solution; 15 h of contact time; 550 rpm of agitation speed (magnetic stirrer); ambient temperature).

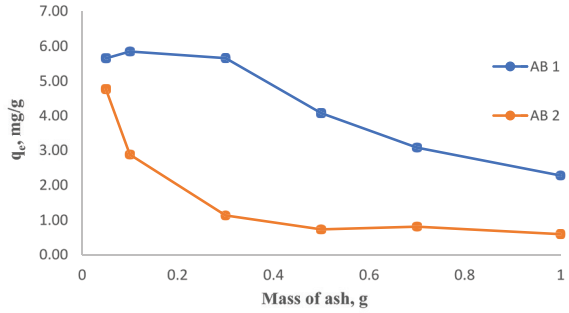

Fig. 18. The effect of fly ash dose on equilibrium capacity of AB 1 and AB 2 for solutions containing 0.05 g L^{-1} of fluoride (50 mL of solution; 15 h of contact time; 550 rpm of agitation speed (magnetic stirrer); ambient temperature).

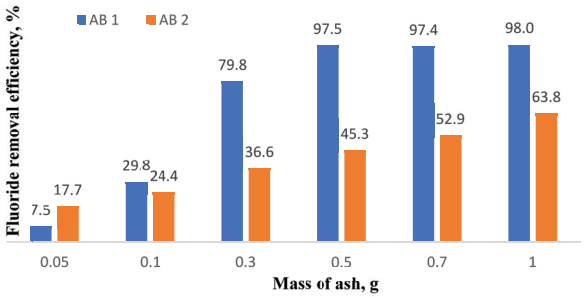

Fig. 19. The effect of ash dose on fluoride removal efficiency for solutions containing 0.5 g L^{-1} of fluoride (50 mL of solution; 15 h of contact time; 550 rpm of agitation speed (magnetic stirrer); ambient temperature).

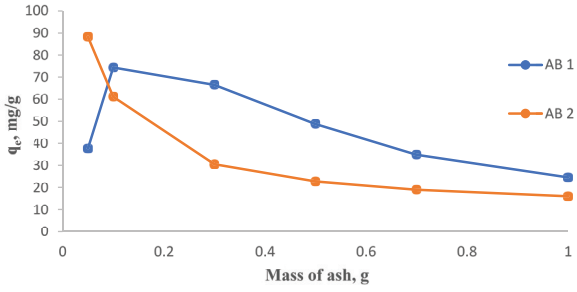

Fig. 20. The effect of fly ash dose on equilibrium capacity of AB 1 and AB 2 for solutions containing 0.5 g L^{-1} of fluoride (50 mL of solution; 15 h of contact time; 550 rpm of agitation speed (magnetic stirrer); ambient temperature).

fly ash increases with the increase of fly ash dose from 0.05 to 0.1 g and then it decreases (Fig. 22), as for 0.5 g L^{-1} solution. The maximal value of about 90 mg g^{-1} is reached both for AB1 and AB 2.

3.2.3. Contact time

The removal of fluoride using the AB 1 ash sample was very high after only 30 min of solid and liquid phase contact, and it raised insignificantly with time up to 180 min and thereafter, it became nearly constant (Fig. 23). In the case of AB 2 sample with the increase of contact time, the removal efficiency constantly raised but after 240 min this accretion was rather small.

The fluoride adsorption capacity of AB 1 reaches value of 47 mg g^{-1} after 30 min, and it increases only to the value of 49 mg g^{-1} after 240 min and it does not change even after mixing the ash and fluoride solution for 900 min (Fig. 24). In the case of AB 2 fly ash sample, the adsorption capacity of 13 mg g^{-1} is reached after 30 min and increases only to the value of 23 mg g^{-1} after 900 min of contact time.

3.2.4. Temperature

The increase of temperature from 298 to 353 K causes a slight increase of fluoride removal on AB 1 fly ash sample, from 74% to 81% (Fig. 25). In the case of AB 2 fly ash sample, the increase of removal efficiency is more significant from 22% to 43%. This shows that the adsorption of fluoride onto fly ash is an endothermic process or it causes the increase of solubility of those fly ash components.

3.2.5. pH

The research done shows that for both fly ash samples, the most effective fluoride removal occurs for the low initial pH of fluoride solution, that is for the value of 2 (Fig. 26). With the increase of pH, the amount of fluoride ions removed decreases and it increases again with increasing the pH to around 10 for AB 1 and for the range of 8–9 for AB 2.

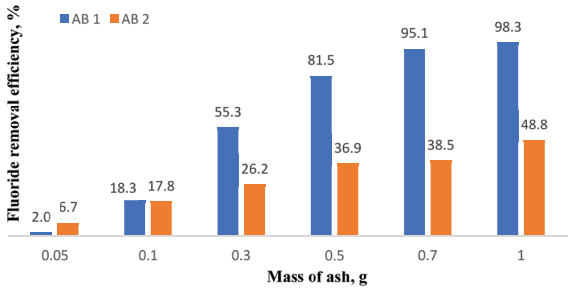

Fig. 21. The effect of fly ash dose on fluoride removal efficiency from solutions containing 1 g L^{-1} of fluoride (50 mL of solution; 15 h of contact time; 550 rpm of agitation speed (magnetic stirrer); ambient temperature).

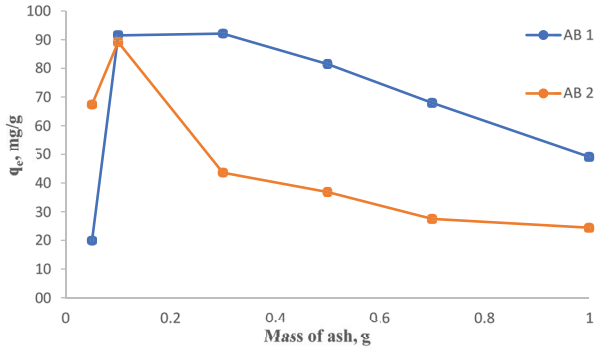

Fig. 22. The effect of fly ash dose on equilibrium capacity of AB 1 and AB 2 for solutions containing 1 g L^{-1} of fluoride (50 mL of solution; 15 h of contact time; 550 rpm of agitation speed (magnetic stirrer); ambient temperature).

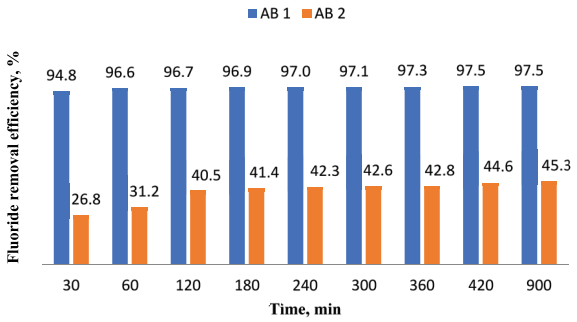

Fig. 23. The effect of contact time of fly ash on fluoride removal efficiency from solutions containing 0.5 g L^{-1} of fluoride (50 mL of solution; 0.5 g of ash; 550 rpm of agitation speed (magnetic stirrer); ambient temperature).

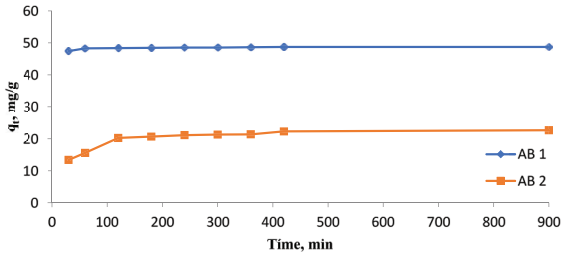

Fig. 24. The effect of contact time on equilibrium capacity of AB 1 and AB 2 for solutions containing 0.5 g L^{-1} of fluoride (50 mL of solution; 0.5 g of ash; 550 rpm of agitation speed (magnetic stirrer); ambient temperature).

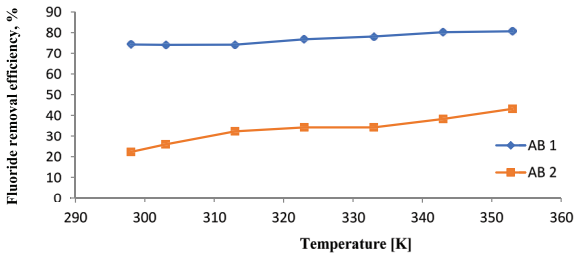

Fig. 25. The effect of temperature on equilibrium capacity of AB 1 and AB 2 for solutions containing 1 g L^{-1} of fluoride (50 mL of solution; 0.5 g of ash; 250 rpm of agitation speed (laboratory shaker with water coat; 0.5 h of contact time).

3.2.6. Agitation rate

The research of agitation speed on fluoride removal efficiency reveal that for both fly ash samples, most of fluoride ions have been removed for the lowest value of agitation rate, i.e., 330 rpm (Fig. 27), irrespective of the initial concentration of fluoride solution. Then, as mixing intensity of the solid and liquid phase increases, for the agitation rate value 550 rpm, the removal efficiency in most cases is significantly reduced. With further increase of agitation speed, an increase in the amount of fluoride ions removed for all examined systems is observed. For the highest value of mixing speed, 1,100 rpm, the removal efficiency decreases again to almost the same value as in the case of 550 rpm for initial concentration of fluoride 1 g L^{-1}, and for lower value in the case of 0.5 g L^{-1}. Almost the same trend has been observed for both of fly ash samples. The smallest impact of the intensity of the mixing speed has been noticed for AB 1, for the initial concentration of the fluoride solution equaling to 0.5 g L^{-1}. It can be generally said that with the increase of agitation rate, the process of their removal changes significantly as it is probably a resultant value of the rivalry of the effect of the change in the solubility of compounds with the ability of fluoride binding together with the effect of the desorption phenomenon occurring along with the increase in the value of the mixing speed.

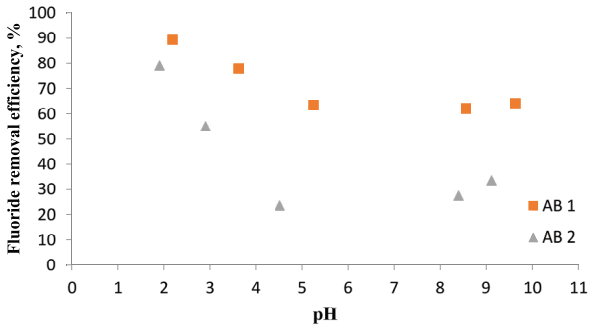

Fig. 26. The effect of pH on equilibrium capacity of AB 1 and AB 2 for solutions containing 1 g L^{-1} of fluoride (50 mL of solution; 0.5 g of ash; 550 rpm of agitation speed (magnetic stirrer), 0.5 h of contact time).

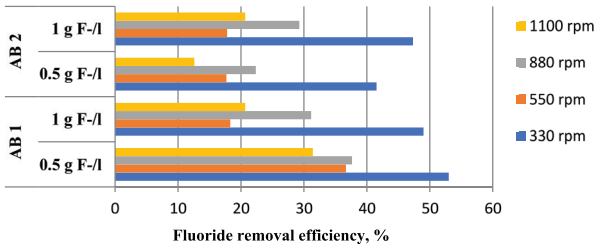

Fig. 27. The effect of agitation rate on equilibrium capacity of AB 1 and AB 2 for solutions containing 0.5 and 1 g L^{-1} of fluoride (50 mL of solution; 0.1 g of ash; 0.5 h of contact time, magnetic stirrer, ambient temperature).

3.2.7. Particle size

As it is shown in Fig. 28, separation of ash AB 1 and AB 2 beads bigger than 32 μ causes an increase in fluoride removal efficiency for both fly ash samples. In case of AB 1 fly ash sample, the increase of amount of fluoride removal has been observed only for solutions that contain lower dose of fly ash regardless of the initial fluoride concentration. For the fly ash dose of 0.1 g, over 2-fold increase of removal efficiency from the value of 18% to the over 38% has been noticed for the initial fluoride concentration 1 g L^{-1}. For an initial concentration of 0.5 g L^{-1}, similar increase in removal efficiency has been noticed. For solutions that contain 0.5 g of fly ash, both for initial fluoride concentration of 0.5 g F^-/L as well as for 1 g F^-/L, the removal efficiency was similar regardless of the ash particle size. In case of AB 2 fly ash sample that contains a lot of bigger beads than the AB 1 ash sample (Figs. 13 and 14), a separation of grains with the particle size lower than 32 μm, causes an increase of fluoride removal efficiency, independently of the dose of fly ash. For the fly ash dose of 0.1 g the increase of removal efficiency is almost the same as for AB 1, over double for the 1 g F^-/L solution, and of about 20% for the 0.5 g F^-/L solution. When the AB 2 ash dose of 0.5 g was used, the increase of about

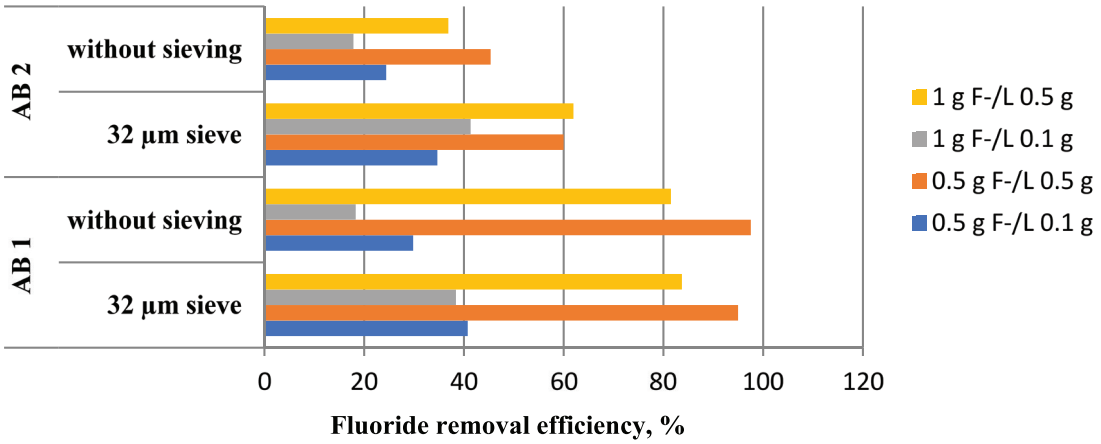

Fig. 28. The effect of particle size of ash samples on equilibrium capacity of AB 1 andAB 2 for solutions containing 0.5 and 1 g L^{-1} of fluoride (50 mL of solution; 15 h of contact time, 550 rpm (magnetic stirrer), ambient temperature).

15% and even 25% was achieved for 0.5 and 1 g L^{-1} of fluoride initial concentration, respectively. Separation of the AB 2 fly ash grains over 32 μm particle size had a very positive effect on a considerable improvement of fluoride removal efficiency of this fly ash.

3.3. Kinetics and adsorption isotherms

The fly ash samples examined contain significant amounts of calcium and small amounts of magnesium which form salts with fluoride ions insoluble in water. As the results of XRD analysis showed, the dominant phase in both of this ash is $CaCO_3$ and some amounts of calcium contained in AB 1 and $CaSO_4$. Only in case of AB 2 ash sample, the solid phase obtained by filtering the rest after mixing the ash with fluoride solution contained some amounts of calcium fluoride, but it was a minor crystal phase that has been recognized. Bearing in mind the above, it is justified to suppose that some amounts of fluoride ions removed from working solutions have been adsorbed by fly ash.

3.3.1. The Kinetic profile of fluoride uptake

From both the ash samples examined, the fitting to plot of fluoride sorption kinetic that was achieved for pseudo-first-order model was weak (Fig. 29). The value of correlation coefficient R^2 that was estimated equaled 0.8837 for AB 1 and 0.8871 for AB 2. In the case of both fly ash samples these values are far away from the desired value of 1. The low conformity of experimental data with the linear plot according to pseudo-first-order model means that the rate of change of solute uptake with time is not directly proportional to the difference in saturation concentration and the amount of solid uptake with time, as was assumed by this model. As the experimental results do not follow this equation, the fluoride sorption onto biomass ash is probably not controlled by diffusion through a boundary in this case.

Significantly better results were obtained by fitting the experimental data to the pseudo-second-order model equation, as the plots of t/qt vs. *t* shown in Fig. 30 indicate. The exact fitting to the pattern of this model is confirmed by the value of correlation coefficient R^2 which equals 1 for AB 1 and 0.9987 for AB 2 ash sample. High compatibility of results achieved with this equation confirms chemisorption involving valency forces through the sharing or exchange of electrons between the adsorbent and adsorbate as covalent force and an ion exchange. The linear regression curves show that the pseudo-second order model provides a better fit to the sorption kinetics data over the whole range of the sorption process for both of fly ash samples.

While considering the Intraparticle surface diffusion model it can be noticed that the fitting to the pattern of model is better for AB 2 than AB 1 (Fig. 31), but neither of the correlation coefficient achieved (0.7425 for AB 1 and 0.8309 for AB 2) is high enough to confirm a mechanism of fluorides adsorption onto these biomass ash samples according to this model. It means that the intraparticle diffusion is not the only rate-limiting step in this case. Moreover, it is also suggested that the process of fluoride adsorption is complex with more than one mechanism limiting the rate of sorption.

3.3.2. Adsorption isotherms

The Langmuir isotherm is the basic isotherm of adsorption. It assumes that the adsorbate can form the surface of the adsorbent molecules interacting with adsorption sites and not interacting (or weakly interacting) with each other. Adsorbent molecules present in the liquid phase have the impact on the surface–the likelihood of their adsorbing rises along with the available free surface. The adsorbed particles show a certain probability of desorption. Both probabilities depend on the temperature and size of the adsorption energy. As the pressure increases, the frequency of particle strokes on the surface increases, and

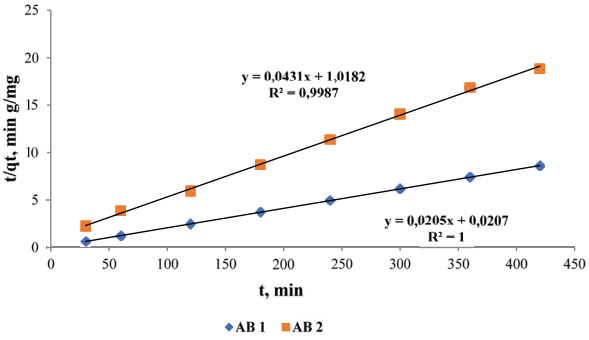

Fig. 30. Pseudo-second-order kinetic fit of fluoride sorption onto fly ash samples AB 1 and AB 2.

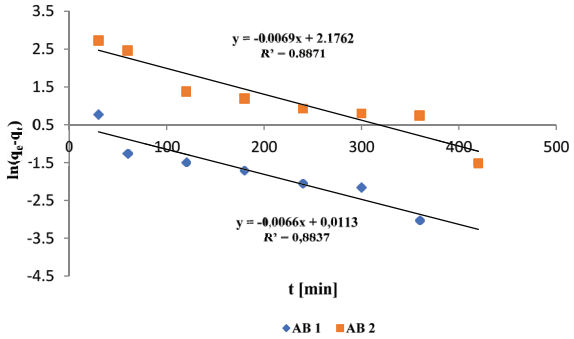

Fig. 29. Pseudo-first-order kinetic fit of fluoride sorption onto biomass fly ash samples AB 1 and AB 2.

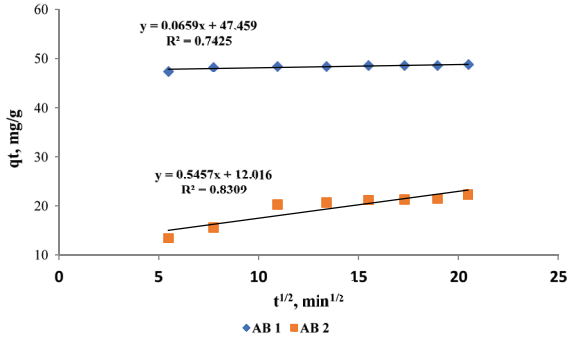

Fig. 31. Intraparticle diffusion model kinetic fit of fluoride sorption onto fly ash samples AB 1 and AB 2.

for the increased amount of adsorbed particles, the available surface decreases. The assumptions for the equation are: the inability form multi-layer, constancy adsorption energy (energetically homogeneous surface) negligible side effects [56].

The Freundlich isotherm is an experimental equation which describes the adsorption on heterogeneous (energetically heterogeneous) surfaces and on microporous adsorbents [56].

Temkin isotherm model assumes that the adsorption occurs onto heterogeneous surface of solid phase. This isotherm corresponds to continuous, infinite (unlimited minimal energy or maximum) energy distribution of the adsorption sites. The equation of the Temkin isotherm assumes that the heat of adsorption of all molecules in the layer decreases linearly due to the adsorbent-adsorbate interaction, and the adsorption is characterized by the even distribution of binding energy [56].

As it can be seen in Figs. 32 and 33, the adsorption equilibrium data of fluoride ions onto biomass ash samples is not fitted very well to the Langmuir isotherm model. The values of coefficient R^2 are 0.6508 and 0.886, for AB 1 and AB 2, respectively. This low compatibility indicates that the adsorption process cannot be characterized by the formation of monolayer coverage on adsorbate as it is assumed by the Langmuir isotherm model.

With relation to the Freundlich isotherm, the fitting to the model equation is slightly better than in the case of Langmuir adsorption model. The correlation coefficient has achieved the value of 0.8152 for AB 1 (Fig. 34) and 0.904 for AB 2 (Fig. 35). However, these values are not high enough to conclude that fluoride adsorption process onto biomass ash is compatible with Freundlich isotherm model.

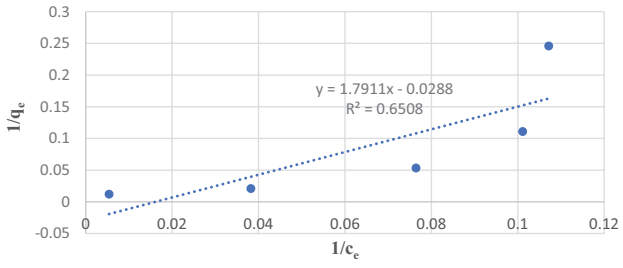

Fig. 32. Langmuir isotherm of fluoride sorption by AB 1.

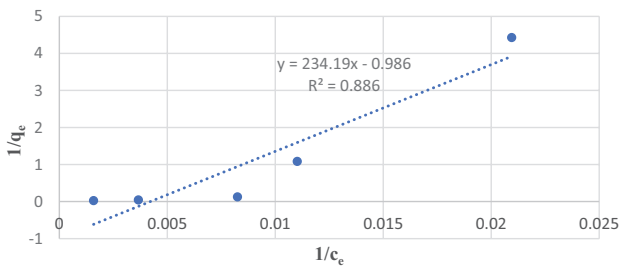

Fig. 33. Langmuir isotherm of fluoride sorption by AB 2.

A very high correlation coefficient by experimental data fitting to the Temkin isotherm model equation with the value of 0.9555 for AB 1 (Fig. 36) and a bit smaller of 0.9508 for AB 2 were achieved (Fig. 37). This good compatibility means that the process of fluoride adsorption onto this ash occurs according to Temkin isotherm model.

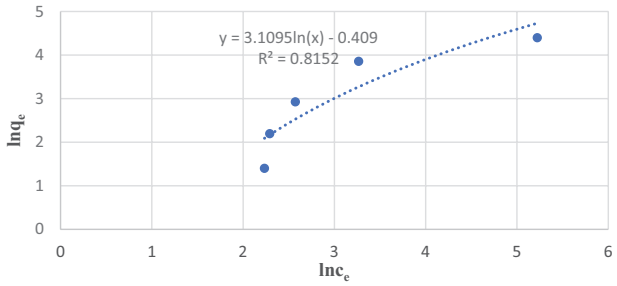

Fig. 34. Freundlich isotherm of fluoride sorption by AB 1.

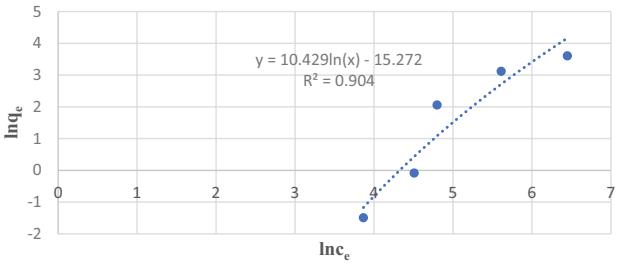

Fig. 35. Freundlich isotherm of fluoride sorption by AB 2.

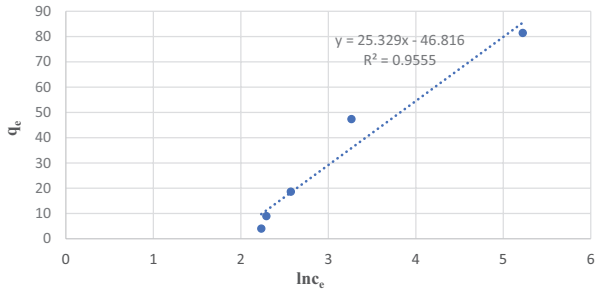

Fig. 36. Temkin isotherm of fluoride sorption by AB 1.

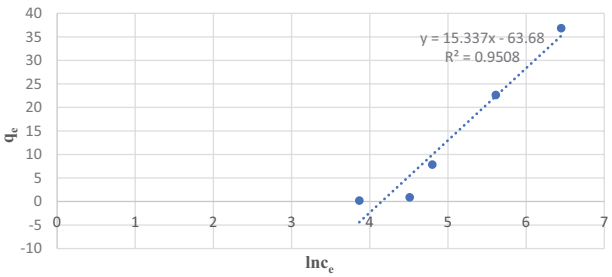

Fig. 37. Temkin isotherm of fluoride sorption by AB 2.

4. Conclusions

It was found that biomass fly ash can be used for fluoride removal material, but its efficiency depends on its chemical composition. Those fly ash samples which contained high content of calcium, sulphates and phosphates turned out to be the most effective. Regarding the total content of Ca in biomass fly ash samples examined (25.98% and 19.3% of CaO for AB 1 and AB 2, respectively) and the fluoride removal efficiency achieved in the preliminary research (50 ml of 5 g F^-/L, 0.5 g of fly ash), i.e., 24.7% and 29.8% for AB 1 and AB 2, respectively, it is obvious that the precipitation of insoluble calcium fluoride is not the only phenomenon responsible for fluoride removal by biomass fly ash. According to results obtained in kinetic research, high compatibility of results achieved with this equation confirmed chemisorption involving valency forces through the sharing or exchange of electrons between the adsorbent and adsorbate as covalent force and an ion exchange.

The porous structure parameters analysis of selected biomass ash samples showed that they have poorly developed specific surface area. Biomass fly ash samples differed in the size of the specific surface area which for AB 1 fly ash sample was four times greater than of AB 2. Almost half of the total pore volume in the measuring range was mesopores, for both ash samples. The pH value of the point of zero charge indicated that the mechanism of fluoride removal by every of biomass fly ash sample was the same for the pH lower than 7.7 and for values higher than 12, because both ash samples are positively charged for that range of pH. As the result of appearance of some amounts of calcium in aqueous soluble form contained in this fly ash, the precipitation of CaF_2 was recognized. The results of XRD analysis of the solid phase after the fluoride removal showed that some crystal phases containing fluoride such as: K_3SO_4F, fluoroapatite $Ca_5(PO_4)_3F$ and hydroxyfluoroapatite $Ca_5(PO_4)_3(OH)_{0.8}F_{0.2}$ was found. However, the phases containing the fluoride with magnesium compounds were not found. The results of FTIR analysis showed that after contact with fluoride solution there were SiF and SiF_2 bonds detected, which indicates the binding of fluorine by silicon compounds present in fly ash.

As the presence of SiO_2 in biomass ash samples has been revealed and the SiF and SiF_2 bonds has been found in FTIR analysis, it can be assumed that one of the major interaction of biomass ash molecule and biomass ash is that that SiO_2 interrelate with water, forming –SiOH group formulations and the adsorption of fluoride is believed to be due to the replacement of F^- for OH^- groups on biomass ash surface.

Another possible hypothesis of interaction of fluoride with biomass ash is fluoride binding by calcium compounds such as calcium carbonate or calcium phosphates according to the reaction schemes presented below.

$$Ca_A(PO_4)_B(OH)_C + D\ F^- = Ca_X(PO_4)_Y{\cdot}(OH)_{2-Z}F_Z + Z\ OH^-$$

$$Ca_A(PO_4)_B{\cdot}CaCO_3 + C\ F^- = Ca_X(PO_4)_Y{\cdot}CaF_2 + Z\ CO_3^{2-}$$

$$CaCO_3 + 2F^- = CaF_2 + CO_3^{2-}$$

There were also found the compounds of potassium sulphates with fluoride in both biomass ash samples.

Two of the fly ash samples that were examined reveal various efficacies in a different range of fluoride concentration. One of them revealed high removal efficacy in the wide range of initial fluoride concentration from 0.05 to 0.5 g L^{-1}. The other one revealed much lower efficiency for this range of fluoride concentration. For both of the fly ash samples, their ability to remove fluoride decreased significantly with the increase of initial fluoride concentration over 0.5 g L^{-1}. Maximal capacity for AB 1, 140 mg g^{-1}, was achieved for 4 g L^{-1} of fluoride solution and 149 mg g^{-1} for AB 2 which was achieved for 5 g L^{-1} of fluoride initial concentration. With an increase of fly ash dose, the removal efficiency increased but the value of equilibrium capacity decreased for the dose over 0.1 g on 50 mL of stock solution. In the case of AB 1, after 30 min of contact time the solid and liquid phase, fluoride removal efficiency was very high and was increased slightly with the extension of this time. For the AB 2, the increase of contact time from 30 to 120 min caused a significant increase of its removal efficiency, but above 120 min that value changed only slightly. The further extension of contact time over 120 min is not economically justified. With the increase of temperature from the ambient value to 353 K, the removal efficiency of AB 1 increased by only 6%, but for AB 2 that value almost doubled. The fluoride removal efficiency was the highest for low pH values of stock solution for both fly ash samples, and it decreased with the increase of that value and it is increases again for over pH = 8. A significant effect of mixing intensity on the fluoride removal ability was observed for both fly ash samples. Particles with size above 32 μm caused a significant increase of fluoride removal ability for AB 2 which contained also bigger particles. In the case of AB 1, efficiency increase after sieving was observed only with low doses of this ash.

The best fit to the sorption kinetics data have been achieved for the Pseudo-Second Order Model for both fly ash samples. High compatibility of results achieved with this equation confirms chemisorption between the adsorbent and adsorbate ion exchange.

Good compatibility in the case AB 1 means that the process of fluoride adsorption onto this ash occurs according to Temkin isotherm model which assumes that adsorption occurs onto heterogeneous surface of solid phase.

The studies described revealed that ash obtained from biomass combustion for energy purposes, can be used as material for fluoride removal with much better affinity for fluoride than coal ash without any pre-treatment, and ash derived from other biomass as well, as it was mentioned in the introduction part. Using of biomass fly ash for the fluoride removal, as the material with good affinity to fluorine, seems to be beneficial especially in the case of wastewaters, when the quality of solution obtained is not as important as in the case of drinking water. In case of industrial wastewaters, it is advisable to use inexpensive materials to remove fluorides, especially waste materials, so as not to increase the operating costs of the purification process.

References

[1] WHO Guidelines for Drinking-Water Quality: Incorporating First Addendum to Third Edition, Vol. 1, Recommendations, Geneva: World Health Organization, 2006.

Available at: http://helid.digicollection.org/en/p/printable.html (Accessed 9 October 2018).
[2] S. Peckham, N. Awofeso, Water fluoridation: a critical review of the physiological effects of ingested fluoride as a public health intervention, Sci. World J., 2014 (2019) 293019.
[3] M. Borysewicz-Lewicka, J. Pydo-Szymaczek, Fluoride in Polish drinking water and the possible risk of dental fluorosis, Pol. J. Environ. Stud., 25 (2016) 9–15.
[4] S. Roy, G. Dass, Fluoride contamination on drinking water – a review, Resour. Environ., 3 (2013) 53–58.
[5] H. Kurosaki, Reduction of fluorine-containing industrial waste using aluminum-solubility method, Oki Tech. Rev., 63 (1998) 53–56.
[6] S. Waghmare, T. Arfin, Fluoride removal from water by various techniques: review, Int. J. Innovative Sci. Eng. Technol., 2 (2015) 560–571.
[7] J. Singh, P. Singh, A. Singh, Fluoride ions vs removal technologies: a study, Arabian J. Chem., 9 (2016) 815–824.
[8] A. Meenakshi, R.C. Maheshwari, Fluoride in drinking water and its removal, J. Hazard. Mater., 137 (2006) 456–463.
[9] M.G. Sujana, R.S. Thakur, S.B. Rao, Removal of fluoride from aqueous solution by using alum sludge, J. Colloid Interface Sci., 206 (1998) 94–101.
[10] W. Nigussie, F. Zewge, B.S. Chandravanshi, Removal of excess fluoride from water using waste residue from the alum manufacturing process, J. Hazard. Mater., 147 (2007) 954–963.
[11] Y. Cengeloglu, E. Kir, M. Ersoz, Removal of fluoride from aqueous solution by using red mud, Sep. Purif. Technol., 28 (2002) 81–86.
[12] A. Tor, N. Danaoglu, G. Arslan, Y. Cengeloglu, Removal of fluoride from water by using granular red mud: batch and column studies, J. Hazard. Mater., 164 (2009) 271–278.
[13] A. Cinarli, O. Bicer, M. Mahramanlioglu, Removal of fluoride using the adsorbentsproduced from mining waste, Fresenius Environ. Bull., 14 (2005) 520–525.
[14] M. Kumari, K. Adhikari, S. Dutta, Fluoride Removal Using Shale: a Mine Waste, Proceedings of India Water Week-Efficient Water Management: Challenges and Opportunities, Government of India, Ministry of Water Resources, Delhi, India, April 08-12, 2013, pp. 157–168.
[15] Y.D. Lai, J.C. Liu, Fluoride removal from water with spent catalysts, Sep. Sci. Technol., 31 (1996) 2791–2803.
[16] C.Y. Tsai, J.C. Liu, Fluoride removal from water with iron-coated spent catalyst, J. Chin. Inst. Environ. Eng., 9 (1999) 107–114.
[17] A.E. Yilmaz, B.A. Fil, S. Bayar, K.Z. Karcioglu, A new adsorbent for fluoride removal: the utilization of sludge waste from electrocoagulation as adsorbent, Global Nest J., 17 (2015) 186–197.
[18] C.K. Geethamani, S.T. Ramesh, R. Gandhimathi, P.V. Nidheesh, Alkali-treated fly ash for the removal of fluoride from aqueous solutions, Desal. Wat. Treat., 52 (2014) 3466–3476.
[19] S.T. Ramesh, R. Gandhimathi, P.V. Nidheesh, M. Taywade, Batch and column operations for the removal of fluoride from aqueous solution using bottom ash, Environ. Res. Eng. Manage., 60 (2012) 12–20.
[20] S.J. Kulkarni, S.R. Dhokpande, J.P. Kaware, Studies on fly ash as an adsorbent for removal of various pollutants from wastewater, Int. J. Eng. Res. Technol., 2 (2013) 1190–1195.
[21] C.K. Geetthamani, S.T. Ramesh, R. Gandhimanti, P.V. Nidheesh, Fluoride sorption by treated fly ash: kinetic and isotherm studies, J. Mater. Cycles Waste Manage., 15 (2013) 381–392.
[22] S. Ranjeeta, Removal of fluoride from drinking water using fly ash after pretreatment, J. Environ. Anal. Toxicol., S7 (2015) 1–3.
[23] D. Goswami, A.K. Das, Removal of fluoride from drinking water using a modified fly ash adsorbent, J. Sci. Ind. Res., 65 (2006) 77–79.
[24] S.V. Vassilev, R. Menendez, Phase-mineral and chemical composition of coal fly ashesas a basis for their multicomponent utilization. 4. Characterization of heavy concentrates and improved fly ash residues, Fuel, 84 (2005) 973–991.
[25] M. Basu, M. Pande, P.B.S. Bhadoria, S.C. Mahapatra, Potential fly-ash utilization in agriculture: a global review, Prog. Nat. Sci., 19 (2009) 1173–1186.
[26] S. Mohan, R. Gandhimathi, Removal of heavy metal ions from municipal solid waste leachate using coal fly ash as an adsorbent, J. Hazard Mater., 169 (2009) 351–359.
[27] A. Bhatnagar, A.K. Minocha, Conventional and non-conventional adsorbents for removal of pollutants from water - a review, Indian J. Chem, Technol., 13 (2006) 203–217.
[28] A.K. Chaturvedi, K.P. Yadava, K.C. Pathak, V.N. Singh, Defluoridation of water by adsorption on fly ash, Water Air Soil Pollut., 49 (1990) 51–61.
[29] P. Xing, L.I. Darvell, J.M. Jones, L. Ma, M. Pourkashanian, A. Williams, Experimental and theoretical methods for evaluating ash properties of pine and El Cerrejon coal used in co-firing, Fuel, 183 (2016) 39–54.
[30] M. Michalik, W. Wilczyńska-Michalik, Mineral and Chemical Composition of Biomass Ash, European Mineralogical Conference, At Frankfurt, Germany, 1 EMC2012-423-1 (2012) doi: 10.13140/2.1.4298.5603.
[31] W.S. Deshmuk, S.J. Attar, M.D. Waghmare, Investigation on sorption of fluoride in water using rice husk as an adsorbent, Nat. Environ. Pollut. Technol., 8 (2009) 217–223.
[32] S. Goyal, A. Sharma, Removal of fluoride from drinking water by natural adsorbent, Int. J. Eng. Res. Technol., 3 (2014) 870–874.
[33] M. Murugan, E. Subramanian, Studies on defluoridation of water by Tamarind seed, an unconventional biosorbent, J. Water Health, 4 (2006) 453–461.
[34] H.A. Sanchez-Sanchez, R. Cortes-Martinez, R. Alfaro-Cuevas-Villanueva, Fluoride removal from aqueous solutions by mechanically modified guava seeds, Int. J. Sci., 11 (2013) 159–172.
[35] N. Ganhdi, D. Sirisha, K.B. Chandra Shekar, Adsorption of fluoride (F^-) from aqueous solution by using pineapple (*Ananas comosus*) peel and orange (*Citrus sinensis*) peel powders, Int. J. Environ. Biorem. Biodegrad., 4 (2016) 55–67.
[36] A. Mohammad, C.B. Majumder, Removal of fluoride from synthetic waste water by using bio-adsorbents, Int. J. Res. Eng. Technol., 3 (2014) 776–786.
[37] D. Mohan, R. Sharma, V.K. Singh, P. Steele, C.U. Pittman Jr, Fluoride removal from water using bio-char, a green waste, low-cost adsorbent: equilibrium uptake and sorption dynamics modelling, Ind. Eng. Chem. Res., 51 (2012) 900–914.
[38] T. Poonam, B. Tanushree, C. Sukalyan, Optimization of fluoride removal from aqueous solution using Jamun (*Syzygium cumini*) leaf ash, Process Saf. Environ., 115 (2018) 125–138.
[39] M. Husain, F.I. Chavan, B. Abhale, Fly ash and maize husk fly ash as an adsorbent for removal of fluoride, Int. J. Sci. Eng. Appl. Sci., 1 (2015) 208–214.
[40] A.S. Jadhav, M.V. Jadhav, Use of mize husk fly ash as an adsorbent for removal of fluoride from water, Int. J. Recent. Dev. Eng. Technol., 2 (2014) 41–45.
[41] N.K. Mondal, R. Bhaumik, T. Baur, B. Das, P. Roy, J.K. Datta, Studies on defluoridation of water by tea ash: an unconventional biosorbent, Chem. Sci. Trans., 1 (2012) 239–256.
[42] V. Ganvir, K. Das, Removal of fluoride from drinking water using aluminium hydroxide coated rice husk ash, J. Hazard. Mater., 185 (2011) 1287–1294.
[43] N.K. Mondal, R. Bhaumik, M.A. Banerjee, J.K. Datta, T. Baur, A comparative study on the batch performance of fluoride adsorption by activated silica gel and activated rice husk ash, Inter. J. Environ. Sci., 2 (2012) 1643–1661.
[44] A.V. Jamode, V.S. Sapkal, V.S. Jamode, Defluoridation of water using inexpensive adsorbents, J. Indian Inst. Sci., 84 (2004) 163–171.
[45] M. Shraboni, H. Gopinath, A review on the sorptive elimination of fluoride from contaminated wastewater, J. Environ. Chem. Eng., 6 (2018) 1257–1270.
[46] H. Cai, G. Chen, C. Peng, Z. Zhang, Y. Dong, G. Shang, X, Zhu, H. Gao, X. Wan, Removal of fluoride from drinking water using tea waste loaded with Al/Fe oxides: a novel, safe and efficient biosorbent, Appl. Surf. Sci., 328 (2015) 34–44.
[47] M. Stolarski, Ł. Graban, S. Szczukowski, J. Tworkowski, Agricultural and forest biomass as feedstock in the manufacture of solid biofuels, Pol. J. Agron., 2 (2010) 67–72.

[48] M.V. Lopez-Ramon, F. Stoeckli, C. Moreno-Castilla, F. Carraso-Marin, On the characterization of acidic and basic surface sites on carbons by various techniques, Carbon, 37 (1999) 1215–1221.
[49] G. Liptay, Atlas of Thermoanalytical Curves, Akademiai Kiado, Budapest, 1973.
[50] NIST Chemistry WebBook.Calcium Carbonate (precipitated). webbook.nist.gov/chemistry.
[51] N.S. Trivedi, S.A. Mandavgane, S. Mehetre, B.D. Kulkarni, Characterization and valorization of biomass ashes, Environ. Sci. Pollut. Res., 23 (2016) 20243–20256.
[52] K.S.W. Sing, D.H. Everett, R.A.W. Haul, L. Moscou, R.A. Pierotti, J. Rouquerol, T. Siemieniewska, Reporting physisorption data for gas/solid systems with special reference to the determination of surface area and porosity, Pure Appl. Chem., 57 (1985) 603–619.
[53] H.K. Naik, Characterization of Fly Ash for Their Effective Management and Utilization, Department of Mining Engineering, 2009–2010, Available online at: http://ethesis.nitrkl.ac.in/1750/1/CHARACTERIZATION_OF_FLY_ASH_FOR_THEIR_EFFECTIVE_MANAGEMENT_AND_UTILIZATIONRakesh_Kumar_Behera%2C_Mining_engg._10605029_(2006–2010)_project.pdf (Accessed 18 October 2018).
[54] M. Repelewicz, K. Jedynak, J. Choma, Porous structure and surface chemistry of activated carbons modified with inorganic acids, Environ. Prot., 31 (2009) 45–50.
[55] E. Paz, N.R. Einat, Z. Yehuda, P. Ze'ev, Determination of the average pore-size and total porosity in porous silicon layers by image processing of SEM micrographs, Microporous Mesoporous Mater., 225 (2016) 465–471.
[56] A.O. Dada, A.P. Olalekan, A.M. Olatunya, Langmuir, Freundlich, Temkin and Dubinin-adushkevich isotherms studies of equilibrium sorption of Zn^{2+} unto phosphoric acid modified rice husk, IOSR J. Appl. Chem., 3 (2012) 38–45.